AD-A102 354 NAVAL SURFACE WEAPONS CENTER SILVER SPRING MD F/G 20/8
CHERENKOV RADIATION FROM A RELATIVISTIC ANNULAR ELECTRON BEAM P--ETC(U)
APR 81 H S UHM
UNCLASSIFIED NSWC/TR-81-139 NL

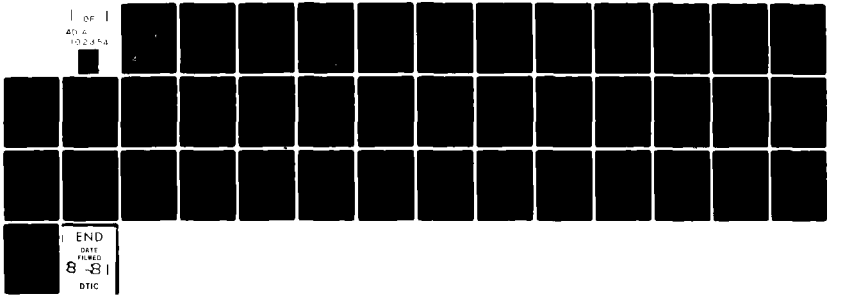

END
DATE FILMED
8-81
DTIC

NSWC TR 81-139

LEVEL II

12

AD A102354

CHERENKOV RADIATION FROM A RELATIVISTIC ANNULAR ELECTRON BEAM PROPAGATING THROUGH A DIELECTRIC LOADED WAVEGUIDE

BY HAN S. UHM

RESEARCH AND TECHNOLOGY DEPARTMENT

FEBRUARY 1981

NAVAL SURFACE WEAPONS CENTER

Dahlgren, Virginia 22448 • Silver Spring, Maryland 20910

UNCLASSIFIED

SECURITY CLASSIFICATION OF THIS PAGE (When Data Entered)

REPORT DOCUMENTATION PAGE	READ INSTRUCTIONS BEFORE COMPLETING FORM
1. REPORT NUMBER: NSWC/TR-81-139	2. GOVT ACCESSION NO.: AD-A102354	3. RECIPIENT'S CATALOG NUMBER
4. TITLE (and Subtitle): CHERENKOV RADIATION FROM A RELATIVISTIC ANNULAR ELECTRON BEAM PROPAGATING THROUGH A DIELECTRIC LOADED WAVEGUIDE .	5. TYPE OF REPORT & PERIOD COVERED: Final rept. - February 1981
	6. PERFORMING ORG. REPORT NUMBER
7. AUTHOR(s): Han S. Uhm	8. CONTRACT OR GRANT NUMBER(s)
9. PERFORMING ORGANIZATION NAME AND ADDRESS: Naval Surface Weapons Center, Code R41, White Oak, Silver Spring, Md. 20910	10. PROGRAM ELEMENT, PROJECT, TASK AREA & WORK UNIT NUMBERS: 0,
11. CONTROLLING OFFICE NAME AND ADDRESS: 12 41	12. REPORT DATE: Apr[redacted]81
	13. NUMBER OF PAGES: 45
14. MONITORING AGENCY NAME & ADDRESS (if different from Controlling Office)	15. SECURITY CLASS. (of this report): UNCLASSIFIED
	15a. DECLASSIFICATION/ DOWNGRADING SCHEDULE

16. DISTRIBUTION STATEMENT (of this Report)

Approved for public release, distribution unlimited

17. DISTRIBUTION STATEMENT (of the abstract entered in Block 20, if different from Report)

18. SUPPLEMENTARY NOTES

19. KEY WORDS (Continue on reverse side if necessary and identify by block number)

Microwave Radiation
Annular Electron Beam
Cherenkov Radiation
Dielectric Waveguide

20. ABSTRACT (Continue on reverse side if necessary and identify by block number)

Stability properties of the free streaming mode (space charge wave) in a relativistic annular electron beam with radius r_0 propagating through a dielectric loaded waveguide is investigated, in connection with the Cherenkov radiation. The stability analysis is carried out within the framework of the linearized Vlasov-Maxwell equations for an electron distribution function, in which all electrons have a Lorentzian distribution in the axial canonical momentum. One of the most important features of the analysis is that, for some ranges of physical parameters, a strong mode coupling between the vacuum

DD FORM 1 JAN 73 1473 EDITION OF 1 NOV 65 IS OBSOLETE S/N 0102-014-6601

UNCLASSIFIED 41156

SECURITY CLASSIFICATION OF THIS PAGE (When Data Entered)

20. dielectric waveguide and free streaming modes occurs, exhibiting possibilities of a Cherenkov radiation. The typical maximum growth rate of instability is a few percent of c/R_0, where c is the speed of light in vacuo. However, the growth rate and bandwidth of instability are substantially reduced by increasing the axial momentum spread.

FOREWORD

Stability properties of the free streaming mode (space charge wave) in a relativistic annular electron beam with radius R_0 propagating through a dielectric loaded waveguide is investigated, in connection with the Cherenkov radiation. The stability analysis is carried out within the framework of the linearized Vlasov-Maxwell equations for an electron distribution function, in which all electrons have a Lorentzian distribution in the axial canonical momentum. One of the most important features of the analysis is that, for some ranges of physical parameters, a strong mode coupling between the vacuum dielectric waveguide and free streaming modes occurs, exhibiting possibilities of a Cherenkov radiation. The typical maximum growth rate of instability is a few percent of c/R_0, where c is the speed of light in vacuo. However, the growth rate and bandwidth of instability are substantially reduced by increasing the axial momentum spread. This research was supported by the Independent Research Fund at the Naval Surface Weapons Center.

H. R. RIEDL
By direction

CONTENTS

ILLUSTRATIONS

ILLUSTRATIONS (CON'T.)

I.

INTRODUCTION

The major recent experimental interest in hollow relativistic electron beams originates from several diverse research areas. One of these areas is the high power microwave generation such as the gyrotron[1,2] relativistic magnetron[3,4] and the free electron lasers.[5,6] In this paper, we present a new promising scheme to produce high power microwave radiation by utilizing relativistic electron beams. The free streaming mode (or the space charge wave) in a relativistic electron beam propagating through a dielectric loaded waveguide exhibits strong instabilities for some ranges of physical parameters. The physical mechanism of instability is typical Cherenkov radiations[7,8] of a charged particle moving through a dielectric material. In this regard, the present paper examines stability properties of the free streaming mode of a hollow relativistic electron beam propagating through a dielectric loaded waveguide, in connection with microwave generation.

The stability analysis is carried out for an annular relativistic electron beam with radius R_0 propagating through a cylindrical waveguide loaded with a dielectric material in range $R_w < r < R_c$, where r is the radial coordinate, R_w is the inner radius of the dielectric material and R_c is the radius of a grounded conducting wall. Equilibrium and stability properties are calculated for the electron distribution

function [Eq. (3)],

$$f_b^0(H, P_\theta, P_z) = \frac{\omega_c N_e \Delta}{4\pi^3 mc^2} \frac{\delta(\gamma-\hat{\gamma})\delta(P_\theta - P_0)}{(P_z - \gamma_b m\beta_b c)^2 + \Delta^2} ,$$

where $H = \gamma mc^2$ is the energy, P_θ is the canonical angular momentum, P_z is the axial canonical momentum, m is the electron rest mass, c is the speed of light in vacuo, $\gamma_b = (1 - \beta_b^2)^{-1/2}$, ω_c, N_e, Δ, $\hat{\gamma}$, and P_0 are constants. The stability analysis of the free streaming mode is carried out within the framework of the linearized Vlasov-Maxwell equations. The formal dispersion relation (17) of the free streaming mode for azimuthally symmetric electromagnetic perturbation ($\partial/\partial\theta = 0$) is obtained in Sec. II, including the important influence of the axial momentum spread (Δ) on stability behavior.

In Sec. III, properties of the vacuum dielectric waveguide mode are investigated without including the influence of beam electrons. It is shown that in the limit of the ratio $R_w/R_c \to 1$ or $\varepsilon \to 1$, where ε is the dielectric constant, the familiar vacuum transverse magnetic (TM) dispersion relation $\omega^2/c^2 - k^2 = \beta_{0n}^2/R_c^2$ in a perfectly conducting waveguide is recovered. Here ω is the eigenfrequency, k is the axial wavenumber and β_{0n} is the nth root of the Bessel function $J_0(\beta_{0n}) = 0$. However, in general, a strong mode coupling between the vacuum dielectric waveguide mode [Eq. (20)]

$$\frac{\omega^2}{c^2} - k^2 = \frac{\xi^2(\omega,k)}{R_w^2} ,$$

and the free streaming mode $\omega = k\beta_b c$ occurs at $k = k_p$ corresponding to the simultaneous solution of these two modes. The parameter $\xi(\omega,k)$ is the root of Eq. (28). By an appropriate choice of ε, the coupling axial wavenumber k_p can be increased to a large number, thereby

substantially enhancing frequencies of the Cherenkov radiation.

Stability properties of the free streaming mode in a dielectric loaded waveguide are investigated. In a range of physical parameters corresponding to instability, the phase velocity of unstable mode is less than the beam velocity, suggesting that the physical mechanism of instability is the Cherenkov radiation.[7] Several points are noteworthy in the analysis in Sec. IV. First, the typical maximum growth rate of instability is few percent of c/R_0, indicating a strong instability. In this regard, we point out that the Cherenkov radiation from an intense hollow electron beam is an effective means for generating a high power microwave. Second, wavelength of the microwave radiation generated by this instability can be typically less than a centimeter for a subcentimeter beam radius. Third, however, the growth rate and bandwidth of instability are substantially reduced by increasing the axial momentum spread.

II.

LINEARIZED VLASOV-MAXWELL EQUATIONS

The present analysis assumes an intense annular electron beam with characteristic thickness 2a and mean radius R_0 propagating through a cylindrical waveguide loaded with a dielectric material in the range $R_w < r < R_c$. The dielectric constant and permeability of the dielectric material are denoted by ε and μ, respectively. A grounded cylindrical conducting wall is located at radius R_c. A strong, externally applied magnetic field $B_0\hat{e}_z$ is needed to confine the beam electrons radially. Cylindrical polar coordinates (r, θ, z) are introduced. To make the analysis tractable, we assume that the thickness of the annular electron beam is much smaller than its mean radius, i.e.,

$$a/R_0 << 1 . \tag{1}$$

Moreover, it is further assumed that

$$\nu/\gamma_b << 1 , \tag{2}$$

where $\nu = N_e e^2/mc^2$ is Budker's parameter, $\gamma_b mc^2$ is the characteristic electron energy, c is the speed of light in vacuo, -e and m are the electron charge and rest mass, respectively, and $N_e = 2\pi \int_0^\infty dr\, r\, n_e^0(r)$ is the number of electrons per unit axial length. Consistent with the low-density assumption in Eq. (2), we neglect the influence of the small equilibrium self-electric and self-magnetic fields that are produced by

the lack of equilibrium charge and current neutralization.

In the present analysis, we investigate stability properties for the choice of equilibrium distribution function

$$f_b^0(H, P_\theta, P_z) = \frac{\omega_c N_e \Delta}{4\pi^3 mc^2} \frac{\delta(\gamma - \hat{\gamma})\delta(P_\theta - P_0)}{(P_z - \gamma_b m\beta_0 c)^2 + \Delta^2} , \tag{3}$$

where $H = \gamma mc^2 = (m^2c^4 + c^2\underset{\sim}{p}^2)^{1/2}$ is the total energy, $P_\theta = r[p_\theta - (e/2c)rB_0]$ is the canonical angular momentum, P_z is the axial canonical momentum, $\omega_c = eB_0/\gamma_b mc$ is the electron cyclotron frequency,

$$P_0 = -(e/2c)(R_0^2 - r_L^2)B_0 , \tag{4}$$

is the canonical angular momentum of an electron with Larmor radius

$$r_L = \frac{c}{\omega_c}[(\hat{\gamma} - \gamma_b)/\gamma_b]^{1/2} , \tag{5}$$

and $\gamma_b = (1 - \beta_b^2)^{-1/2}$ and Δ are constants.

In the subsequent analysis, use is made of the linearized Vlasov-Maxwell equations for azimuthally symmetric perturbations ($\partial/\partial\theta = 0$) about a tenuous hollow beam equilibrium described by Eq. (3). We adopt a normal-mode approach in which all perturbations are assumed to vary according to

$$\delta\psi(\underset{\sim}{x},t) = \hat{\psi}(r)\exp[i(kz - \omega t)] ,$$

where $\mathrm{Im}\omega > 0$. Here, ω is the complex eigenfrequency and k is the axial wavenumber. The Maxwell equations for the perturbed electric and magnetic field amplitudes can be expressed as

$$\begin{aligned} \underset{\sim}{\nabla} \times \hat{\underset{\sim}{E}}(\underset{\sim}{x}) &= i(\omega/c)\hat{\underset{\sim}{B}}(\underset{\sim}{x}) , \\ \underset{\sim}{\nabla} \times (1/\mu)\hat{\underset{\sim}{B}}(\underset{\sim}{x}) &= (4\pi/c)\hat{\underset{\sim}{J}}(\underset{\sim}{x}) - i(\omega/c)\epsilon\hat{\underset{\sim}{E}}(\underset{\sim}{x}) , \end{aligned} \tag{6}$$

where ϵ and μ are the dielectric constant and permeability, respectively, $\hat{\underset{\sim}{E}}(\underset{\sim}{x})$ and $\hat{\underset{\sim}{B}}(\underset{\sim}{x})$ are the perturbed electric and magnetic fields, and

$$\hat{\underset{\sim}{J}}(\underset{\sim}{x}) = -e\int d^3p\ \underset{\sim}{v}\ \hat{f}_b(\underset{\sim}{x},\underset{\sim}{p}) \ , \tag{7}$$

is the perturbed current density. Note that $\epsilon = \mu = 1$ in <u>vacuo</u>. In Eq. (7),

$$\hat{f}_b(\underset{\sim}{x},\underset{\sim}{p}) = e\int_{-\infty}^{0} d\tau\ \exp(-i\omega\tau)\left[\hat{\underset{\sim}{E}}(\underset{\sim}{x}') + \frac{\underset{\sim}{v}' \times \hat{\underset{\sim}{B}}(\underset{\sim}{x}')}{c}\right]\frac{\partial}{\partial \underset{\sim}{p}'} f_b^0 \ , \tag{8}$$

is the perturbed distribution function, $\tau = t' - t$, and the particle trajectories $\underset{\sim}{x}'(t')$ and $\underset{\sim}{p}'(t')$ satisfy $d\underset{\sim}{x}'/dt' = \underset{\sim}{v}'$ and $d\underset{\sim}{p}'/dt' = -e\underset{\sim}{v}' \times B_0\hat{\underset{\sim}{e}}_z/c$, with "initial" conditions $\underset{\sim}{x}'(t' = t) = \underset{\sim}{x}$ and $\underset{\sim}{v}'(t' = t) = \underset{\sim}{v}$.

In general, the permeability μ of a dielectric material even in the wall differs from unity by only a few parts in 10^5. Therefore, we approximate $\mu = 1$ in the remainder of this paper. Making use of Eq. (6), it is straightforward to show that

$$\hat{E}_r(r) = (kc/\omega\epsilon)\hat{B}_\theta(r) \ ,$$

$$\hat{B}_\theta(r) = i[\omega\epsilon/c(\omega^2\epsilon/c^2 - k^2)][\partial\hat{E}_z(r)/\partial r] \ , \tag{9}$$

and

$$\left(\frac{1}{r}\frac{\partial}{\partial r}\, r\, \frac{\partial}{\partial r} + \frac{\omega^2}{c^2}\,\epsilon - k^2\right)\hat{E}_z(r) = 4\pi ik\left[\hat{\rho}(r) - \frac{\omega}{c^2 k}\,\hat{J}_z(r)\right] \ , \tag{10}$$

where $\hat{B}_\theta$ is the azimuthal component of the perturbed magnetic field, and $\hat{E}_r$ and $\hat{E}_z$ are the radial and axial components, respectively, of the perturbed electric field, $\hat{\rho}(r)$ is the perturbed charge density and $\hat{J}_z(r)$ is the axial component of the perturbed current density.

To lowest order, the axial motion of the particle orbit is free-

streaming,

$$z' = z + \frac{p_z}{\gamma m} (t' - t) \ . \tag{11}$$

Moreover, within the context of Eq. (2), we neglect the terms proportional to $\hat{E}_\perp(r)$ in the right-hand side of Eq. (8), where $\hat{E}_\perp(r)$ is the transverse component of the perturbed electric field. Finally, since the oscillatory modulation of the radial orbit is small [Eq. (1)], we approximate $r' \simeq r$ in the arguments of the perturbation amplitudes on the right-hand side of Eq. (8).

Substituting Eq. (11) into Eq. (8) and carrying out the momentum integration, it can be shown for $0 < r < R_w$ that Eq. (10) is expressed as

$$\left(\frac{1}{r}\frac{\partial}{\partial r} r \frac{\partial}{\partial r} + p_1^2\right)\hat{E}_z(r) = - \frac{\delta(r - R_0)}{R_0} \sigma(\omega,k)\hat{E}_z(r) \ , \tag{12}$$

where the source function $\sigma(\omega,k)$ is defined by

$$\sigma(\omega,k) = \frac{2\nu}{\gamma_b^3} \frac{k^2c^2 - \omega^2}{(\omega - k\beta_b c + ik\Delta/\gamma_b^3 m)^2} \ , \tag{13}$$

and

$$p_1^2 = \omega^2/c^2 - k^2 \ . \tag{14}$$

In obtaining Eq. (12), use has been made of Eq. (1). For a detailed derivation of Eq. (12), we recommend the reader to review the previous literature.[6]

For the convenience in the future analysis, we define the wave impedance $Z(\omega,k)$ of the wall as

$$Z(\omega,k) = -i(\omega R_w/c) \frac{\hat{E}_z(R_w)}{\hat{B}_\theta(R_w)} \ , \tag{15}$$

at the surface of the dielectric material $r = R_w$. Evidently, the solutions to Eq. (12) are given by

$$\hat{E}_z(r) = \begin{cases} AJ_0(p_1 r) , & 0 \leq r < R_0 , \\ BJ_0(p_1 r) + CN_0(p_1 r) , & R_0 < r \leq R_w , \end{cases} \tag{16}$$

where $J_\ell(x)$ and $N_\ell(x)$ are Bessel functions of the first and second kind, respectively, of order ℓ. Making use of Eqs. (9) and (15) and the boundary conditions of $\hat{E}_z(r)$ at $r = R_0$, we obtain the dispersion relation

$$\frac{2\nu}{\gamma_b^3} \frac{k^2c^2 - \omega^2}{(\omega - k\beta_b c + ik\Delta/\gamma_b^3 m)^2} = F(\omega,k) , \tag{17}$$

where $F(\omega,k)$ is the wave admittance at the beam location defined by

$$F(\omega,k) = -\frac{2}{\pi} \frac{g(\xi)/J_0(p_1R_0)}{J_0(p_1R_0) + g(\xi)N_0(p_1R_0)} . \tag{18}$$

In Eq. (18),

$$g(\xi) = \frac{J_1(\xi)}{\xi N_0(\xi) - ZN_1(\xi)} \left[Z - \frac{\xi J_0(\xi)}{J_1(\xi)} \right] , \tag{19}$$

and the parameter ξ is defined by

$$\frac{\omega^2}{c^2} - k^2 = \frac{\xi^2}{R_w^2} . \tag{20}$$

Approximating the permeability of a dielectric material $\mu = 1$, we note that the perturbed axial electric field $\hat{E}_z(r)$ and azimuthal magnetic field $\hat{B}_\theta(r)$ are continuous across the dielectric boundary at $r = R_w$. From Eq. (10), we obtain

$$\left(\frac{1}{r} \frac{\partial}{\partial r} r \frac{\partial}{\partial r} + p_2^2 \right) \hat{E}_z(r) = 0 , \tag{21}$$

inside the dielectric material ($R_w \leq r \leq R_c$). Here p_2 is defined by

$$p_2^2 = \omega^2\varepsilon/c^2 - k^2 . \tag{22}$$

The solution to Eq. (21) can be expressed as

$$\hat{E}_z(r) = A[J_0(p_2 r) - J_0(p_2 R_c)N_0(p_2 r)/N_0(p_2 R_c)] \ , \qquad (23)$$

where A is an arbitrary constant. Substituting Eq. (23) into Eq. (9), and making use of the boundary condition in Eq. (15) at $r = R_w$, we obtain the impedance,

$$Z = \frac{\eta}{\epsilon} \frac{J_0(\eta)N_0(\eta R_c/R_w) - J_0(\eta R_c/R_w)N_0(\eta)}{J_1(\eta)N_0(\eta R_c/R_w) - J_0(\eta R_c/R_w)N_1(\eta)} \ , \qquad (24)$$

at the surface of dielectric material $r = R_w$. In Eq. (24), the parameter η is defined by

$$\frac{\omega^2}{c^2}\epsilon - k^2 = \frac{\eta^2}{R_\omega^2} \ . \qquad (25)$$

Equation (17), when combined with Eqs. (18), (19), and (24), yields a closed dispersion relation for the Cherenkov radiation of a hollow electron beam in a dielectric loaded waveguide. In the remainder of this article, we make use of Eq. (17) to investigate properties of the Cherenkov radiation for a broad range of physical parameters.

III.

VACUUM DIELECTRIC WAVEGUIDE MODES

Before going through the stability analysis of Eq. (17), we investigate properties of the vacuum dielectric waveguide modes characterized by

$$\nu/\gamma_b \to 0 \ . \tag{26}$$

In this limit, the vacuum dielectric dispersion relation is given by Eq. (20), where the parameter $\xi(\omega,k)$ is the root of

$$g(\xi) = 0 \ . \tag{27}$$

Substituting Eq. (19) into Eq. (27), we can show that Eq. (27) is equivalently expressed as

$$\begin{aligned} Z &= \frac{\xi J_0(\xi)}{J_1(\xi)} \\ &= \frac{\eta}{\epsilon} \frac{J_0(\eta)N_0(\eta R_c/R_w) - J_0(\eta R_c/R_w)N_0(\eta)}{J_1(\eta)N_0(\eta R_c/R_w) - J_0(\eta R_c/R_w)N_1(\eta)} \ , \end{aligned} \tag{28}$$

which relates the parameter ξ to η. Equation (28) with Eqs. (20) and (25) gives a complete dispersion relation for the vacuum dielectric waveguide modes.

It is instructive to examine Eq. (28) in the limit $\epsilon \to 1$. Making use of $\eta = \xi$, we obtain

$$J_0(\xi R_c/R_w) = 0 \ , \tag{29}$$

which gives the familiar vacuum transverse magnetic (TM) dispersion relation

$$\frac{\omega^2}{c^2} - k^2 = \frac{\beta_{0n}^2}{R_c^2} , \tag{30}$$

in a perfectly conducting waveguide. Moreover, we can show that in the limit of both $R_w \to R_c$ and $R_w \to 0$, Eq. (28) gives the dispersion relation in Eq. (30) and

$$\frac{\omega^2}{c^2}\,\varepsilon - k^2 = \frac{\beta_{0n}^2}{R_c^2} , \tag{31}$$

respectively. Note that the case $R_w \to 0$ corresponds to a completely filled dielectric waveguide.

For given values of the dielectric constant ε and the ratio R_w/R_c, the parameter ξ is determined from Eq. (28) in terms of η. The oscillation frequency ω and axial wavenumber k in a vacuum dielectric loaded waveguide are obtained from the simultaneous solution of Eqs. (20) and (25) for specified ξ and η. Figure 1 is plot of the vacuum dielectric dispersion relation in the parameter space (ω,k) for (a) $R_w/R_c = 0.8$ and several values of the dielectric constant ε, and (b) $\varepsilon = 4$ and several values of the ratio R_w/R_c. We remind the reader that the thickness of dielectric material increases from zero to R_c as the ratio R_w/R_c decreases from unity to zero. Plot in Fig. 1 corresponds to the first radial mode number $n = 1$. The dispersion curve for $R_w/R_c = 0$ in Fig. 1(b) represent the dispersion relation of a completely filled dielectric waveguide [Eq. (31)]. On the other hand, the curves for $\varepsilon = 1$ in Fig. 1(a) and for $R_w/R_c = 1$ in Fig. 1(b) correspond to the ordinary TM mode dispersion relation in Eq. (30) where the phase

velocity $V_{ph} = \omega/k$ is always faster than the speed of light ($\omega/k > c$). However, the phase velocity of the dispersion relation in a dielectric loaded waveguide is sometimes less than the speed of light ($\omega/k < c$). For example, for $R_w/R_c = 0.8$ and $\varepsilon = 4$ in Fig. 1(a), we find $\omega/k > c$ for $kR_c < 3.3$ and $\omega/k < c$ for $kR_c > 3.3$.

Shown in Fig. 2 is a schematic plot of $\omega = (k^2c^2 + \beta_{0n}^2 c^2/R_c^2)^{1/2}$ versus k corresponding to a perfectly conducting waveguide and $\omega = (k^2c^2 + \xi^2 c^2/R_w^2)^{1/2}$ versus k corresponding to a dielectric loaded waveguide. The straight line $\omega = k\beta_b c$ represents the free-streaming mode. In a range of physical parameters, the mode $\omega = k\beta_b c$ intersects the curve $\omega = (k^2c^2 + \xi^2 c^2/R_w^2)^{1/2}$ at $k = k_p$, indicating a possible mode coupling. In fact, for $k > k_p$ in Fig. 2, the phase velocity of the vacuum dielectric mode is less than the beam velocity. In this regard, we expect a strong Cherenkov radiation[7,8] near the intersection point k_p of these two modes. Figure 3 is plot of k_pR_c versus ε obtained from simultaneous solution of $\omega = k\beta_b c$ and $\omega = [k^2c^2 + \xi^2(\omega,k)c^2/R_w^2]^{1/2}$ for $R_w/R_c = 0.8$ and several values of the electron energy γ_b. Obviously, the value of k_pR_c increases considerably as the dielectric constant ε decreases. For example, for $\gamma_b = 1.5$, $k_pR_c = 4.25$ for $\varepsilon = 8$ and $k_pR_c = 20$ for $\varepsilon = 2.05$. In this regard, the Cherenkov radiation frequency can be substantially enhanced by an appropriate choice of the dielectric material.

IV.

STABILITY ANALYSIS OF FREE-STREAMING MODES

In this section, we investigate stability properties of the free-streaming mode (or the space charge wave) $\omega = k\beta_b c$ in a dielectric loaded waveguide, in connection with the Cherenkov radiation. Making use of the fact that the Doppler-shifted eigenfrequency $\omega - k\beta_b c$ is well removed from the free-streaming mode, i.e., $|\omega - k\beta_b c| \ll k\beta_b c$, and evaluating the parameters ξ and η, and the wave admittance F in Eq. (18) at $\omega = \omega_0 = k\beta_b c$, the dispersion relation in Eq. (17) can be approximated by

$$\left(\omega - k\beta_b c + i\,\frac{k\Delta}{\gamma_b^3 m}\right)^2 [F_0 + (dF/d\omega)_{\omega_0}(\omega - k\beta_b c)] = \frac{2\nu}{\gamma_b^3}(k^2c^2 - \omega^2) , \tag{32}$$

where

$$F_0 = F(\omega_0, k) . \tag{33}$$

Defining the normalized Doppler-shifted eigenfrequency Ω by

$$\Omega = (\omega - k\beta_b c)R_0/c , \tag{34}$$

the dispersion relation in Eq. (32) is numerically investigated for a broad range of physical parameters. For present purposes, to illustrate the mode coupling of the free-streaming mode ($\omega = k\beta_b c$) with the vacuum dielectric waveguide mode, shown in Fig. 4 are plot of (a) F_0 (solid curve) and $(c/R_0)(dF/d\omega)_{\omega_0}$ (dashed curve) and (b) the normalized

growth rate $\Omega_i = \mathrm{Im}\Omega$ versus kR_0 obtained from Eqs. (18), (19), (24), and (32) for $\gamma_b = 2$, $\varepsilon = 8$, $R_0/R_w = 0.8$, $R_w/R_c = 0.8$, $\nu = 0.002$ and several values of Δ. Several points are noteworthy in Fig. 4. First, the maximum growth rate of instability for a relativistic electron beam ($\gamma_b \gtrsim 1.5$) occurs at $k = k_p$ satisfying $F_0(k_p) = 0$, where k_p is the mode coupling point in Figs. 2 and 3. For example, in Fig. 4, the maximum coupling occurs at $kR_0 = 3.35$. Second, the typical maximum growth rate is five percent of c/R_0, indicating a strong instability. In this regard, this instability can be utilized to produce intense microwave radiation. Third, a typical wavelength of the microwave radiation generated by this instability can be less than a centimeter for a subcentimeter beam radius. Fourth, the growth rate and bandwidth of instability decrease with an increasing value of the axial momentum spread. Finally, from the numerical calculation, we note that the Doppler-shifted real frequency $\Omega_r = \mathrm{Re}\Omega$ for instability is negative, thereby implying that the phase velocity of unstable modes is less than the beam velocity. We therefore conclude that the instability mechanism is a typical Cherenkov radiation.[7,8]

Of considerable interest for experimental applications is the stability behavior for specified values of the ratios R_w/R_c and R_0/R_w and several values of the dielectric constant ε. Typical results are shown in Fig. 5 where Ω_i is plotted versus kR_0 for $\Delta = 0$ and parameters otherwise identical to Fig. 4. Note that the eigenfrequency ω of instability is approximated by $\omega \simeq k\beta_b c$. In this regard, by an appropriate choice of the dielectric material (ε), we can considerably enhance the excitation frequency of the microwave radiation. For example, in Fig. 5, the maximum growth rate of instability occurs at $kR_0 = 2.25$ for

$\varepsilon = 6$ and at $kR_0 = 5.2$ for $\varepsilon = 2$, which is consistent with the results in Fig. 3. The dependence of stability properties on the ratio R_0/R_w is further illustrated in Fig. 6, where the normalized growth rate $\Omega_i = \mathrm{Im}\Omega$ is plotted versus kR_0 for $\Delta = 0$, $\varepsilon = 3$, and parameters otherwise identical to Fig. 4. Obviously from Fig. 6, we note that the growth rate and bandwidth of instability increase rapidly as the surface of dielectric material approaches to the beam surface ($R_0/R_w \to 1$) for a given beam radius.

We now examine the case where the electron beam energy is mildly relativistic ($\gamma_b = 1.15$). Figure 7 shows plots of (a) F_0 (solid curve) and $(c/R_0)(dF/d\omega)_{\omega_0}$ (dashed curve), and (b) the normalized growth rate $\Omega_i = \mathrm{Im}\Omega$ versus kR_0 obtained from Eqs. (18), (19), (24), and (32) for $\gamma_b = 1.15$, $\varepsilon = 20$, $R_0/R_w = 0.8$, $R_w/R_c = 0.8$, $\Delta = 0$, and $\nu = 0.002$. Comparing Fig. 7(a) with Fig. 4(a), we find that the wave admittance F for a small energy beam is a fast varying function of kR_0. In this regard, the approximation in Eq. (32) for a small energy beam is less valid than that for a relativistic electron beam ($\gamma_b \gtrsim 1.5$). For example, in Fig. 7(b), the numerical results of the growth rate in range $2.17 < kR_0 < 2.33$ is not accurate. In the remainder of this article, we therefore ignore a small growth rate bump like this. In contrast with Fig. 4, the axial wavenumber corresponding to the maximum growth rate deviates substantially from $k = k_p$ satisfying $F_0(k_p) = 0$. For example, for $\gamma_b = 1.15$ in Fig. 7, $k_pR_0 = 2.53$. On the other hand, the maximum growth rate of instability occurs at $kR_0 = 2.62$. However, the typical maximum growth rate of instability is again five percent of c/R_0.

An example is investigated to illustrate influence of axial momentum

spread on stability behavior for a mildly relativistic electron beam ($\gamma_b = 1.15$). Figure 8 shows plot of the normalized growth rate Ω_i versus kR_0 obtained from Eq. (32) for several values of Δ and parameters otherwise identical to Fig. 7. Evidently, the growth rate of instability decreases substantially with an increasing value of axial momentum spread. Shown in Fig. 9 is plot of the normalized growth rate versus kR_0 obtained from Eq. (32) for $\Delta = 0$, several values of dielectric constant ε, and parameters otherwise identical to Fig. 7. Similarly to the results in Fig. 5, we can enhance frequency of the microwave radiation by an appropriate choice of the dielectric material (ε). Moreover, the maximum growth rate of instability also increases by appropriately decreasing values of dielectric constant ε.

V.

CONCLUSIONS

In this paper, we have examined stability properties of the free-streaming mode ($\omega = k\beta_b c$) in a relativistic annular electron beam propagating through a dielectric loaded waveguide, in connection with the Cherenkov radiation. The stability analysis was carried out within the framework of the linearized Vlasov-Maxwell equations, assuming that the electron beam is thin ($a/R_0 << 1$) and that $\nu/\gamma_b << 1$. Stability properties were calculated for the electron distribution function in which all electrons have a Lorentzian distribution in the axial canonical momentum. In this regard, the influence of the axial momentum spread on stability behavior can be also investigated. The formal dispersion relation of the free-streaming mode for azimuthally symmetric electromagnetic perturbations ($\partial/\partial\theta = 0$) was obtained in Sec. II. Properties of the vacuum dielectric waveguide mode were investigated in Sec. III, without including the influence of beam electrons. It was shown in Sec. III that in general, a mode coupling between the vacuum dielectric waveguide mode and the free-streaming mode occurs at a range of physical parameters, exhibiting possibilities of a strong Cherenkov radiation. Stability properties of the free-streaming mode for a dielectric loaded waveguide were investigated in Sec. IV. It was found that the maximum growth rate of instability is a few percent of c/R_0. In this context, the Cherenkov radiation from a relativistic annular electron beam can

be an effective means for producing intense high power microwave. Wavelength of the microwave radiation can be less than a centimeter.

ACKNOWLEDGMENTS

This research was supported by the Independent Research Fund at the Naval Surface Weapons Center.

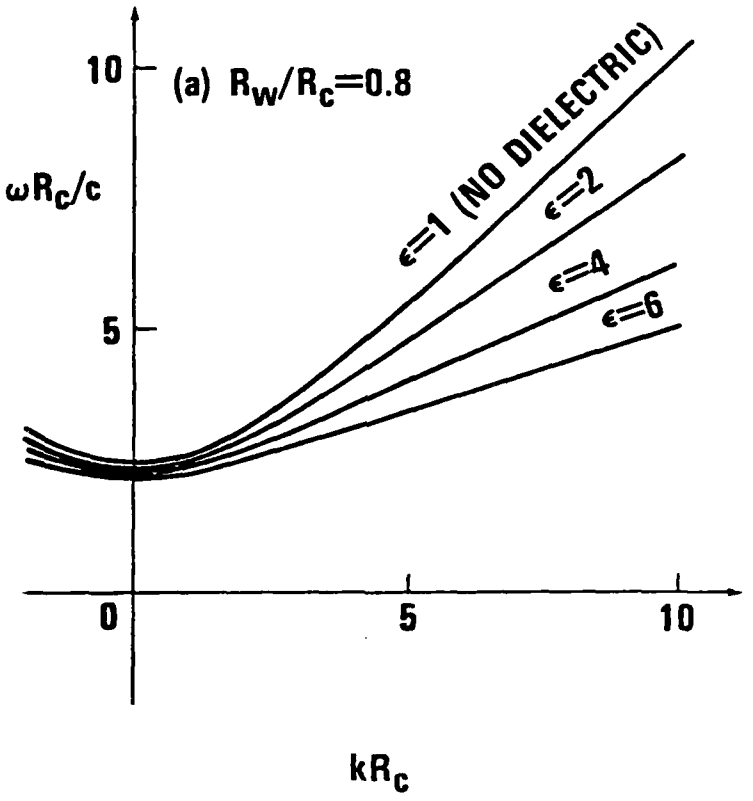

FIGURE 1a PLOT OF THE VACUUM DIELECTRIC WAVEGUIDE MODE IN THE PARAMETER SPACE (ω,k) OBTAINED FROM EQS. (20), (25), AND (28).

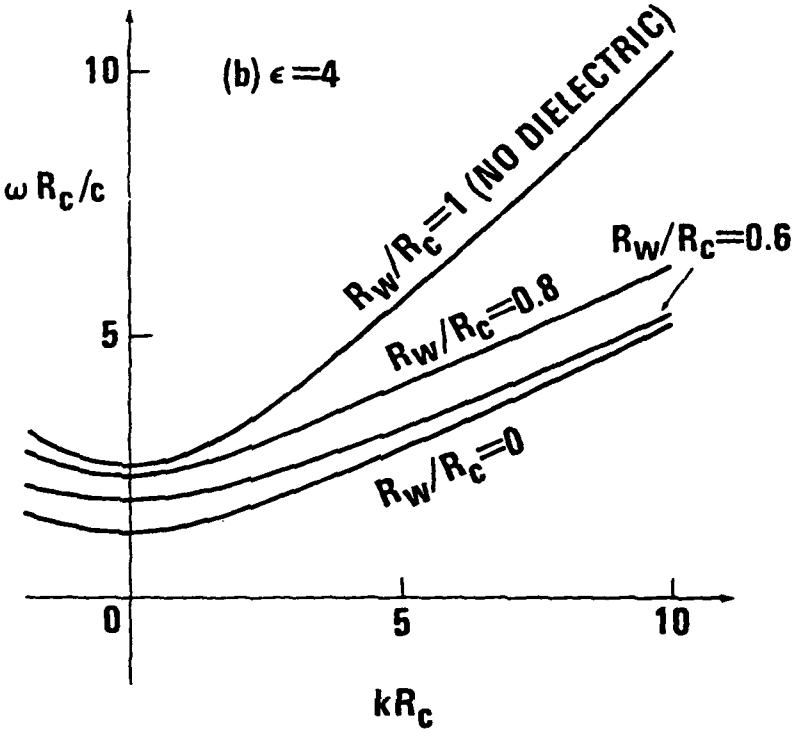

FIGURE 1b R_w/R_c = 0.8 AND SEVERAL VALUES OF THE DIELECTRIC CONSTANT ϵ = 4 AND SEVERAL VALUES OF THE RATIO R_w/R_c.

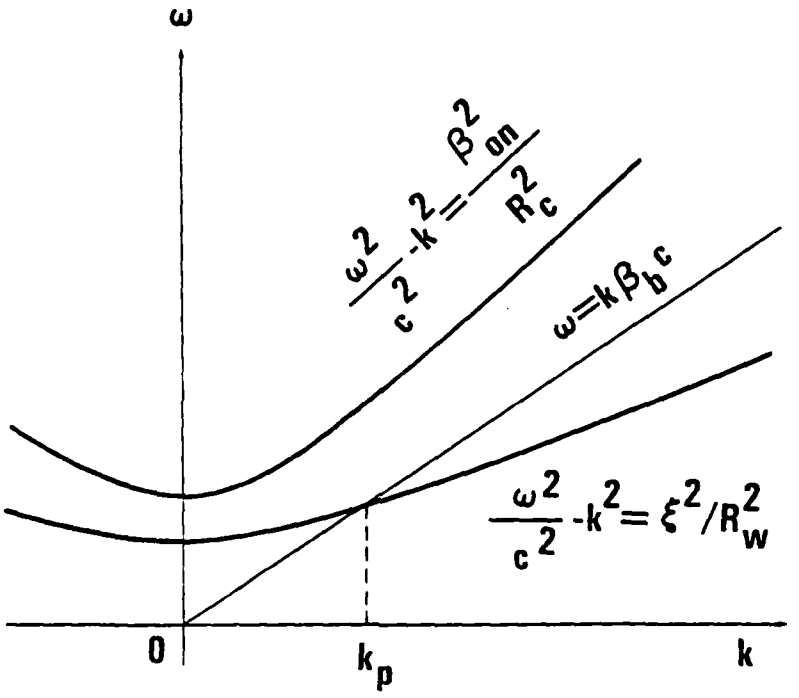

FIGURE 2 SKETCH OF $\omega = (k^2c^2 + \beta_{On}^2 c^2/R_c^2)^{1/2}$ VERSUS K (CORRESPONDING TO PERFECTLY CONDUCTING WAVEGUIDE) AND $\omega = (k^2c^2 + \xi^2c^2/R_w^2)^{1/2}$ VERSUS k (CORRESPONDING TO A DIELECTRIC LOADED WAVEGUIDE). THE STRAIGHT LINE $\omega = k\beta_b c$ IS THE FREE STREAMING MODE.

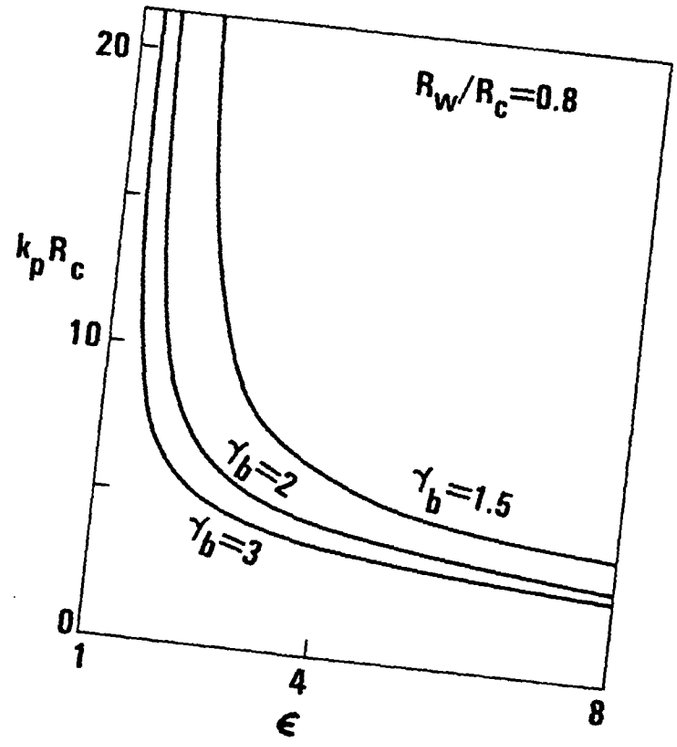

FIGURE 3 PLOT OF THE NORMALIZED COUPLING AXIAL WAVENUMBER k_pR_c VERSUS ϵ OBTAINED FROM $\omega = K\beta_{bc}$ AND EQ. (20) FOR $R_w/R_c = 0.8$ AND SEVERAL VALUES OF THE ELECTRON ENERGY γ_b.

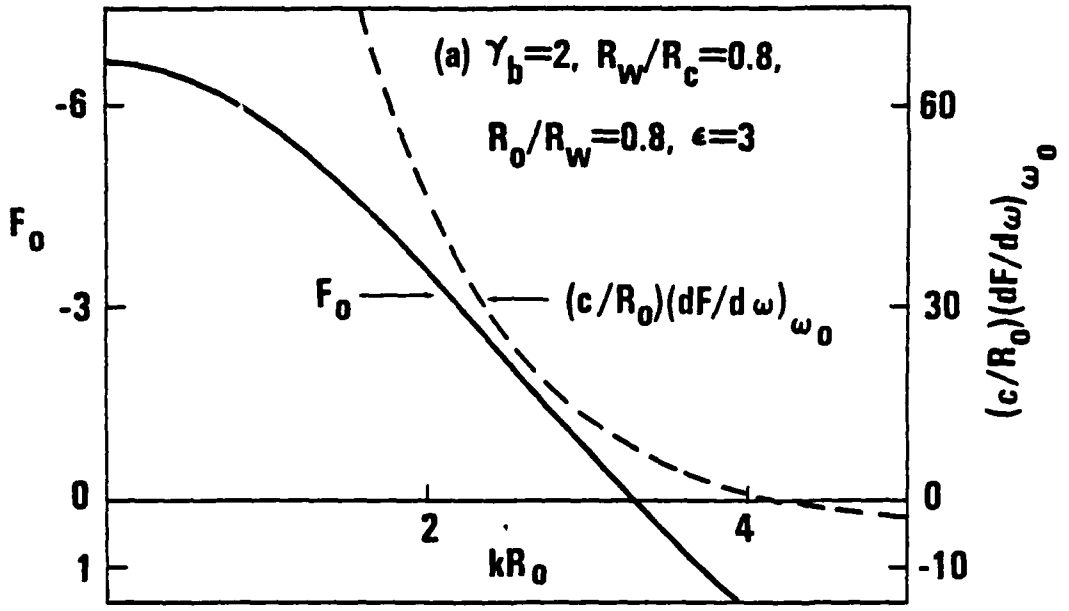

FIGURE 4a PLOT OF (a) F_0 (SOLID CURVE) AND $(c/R_0)\,(dF/d\omega)_{\omega 0}$ (DASHED CURVE).

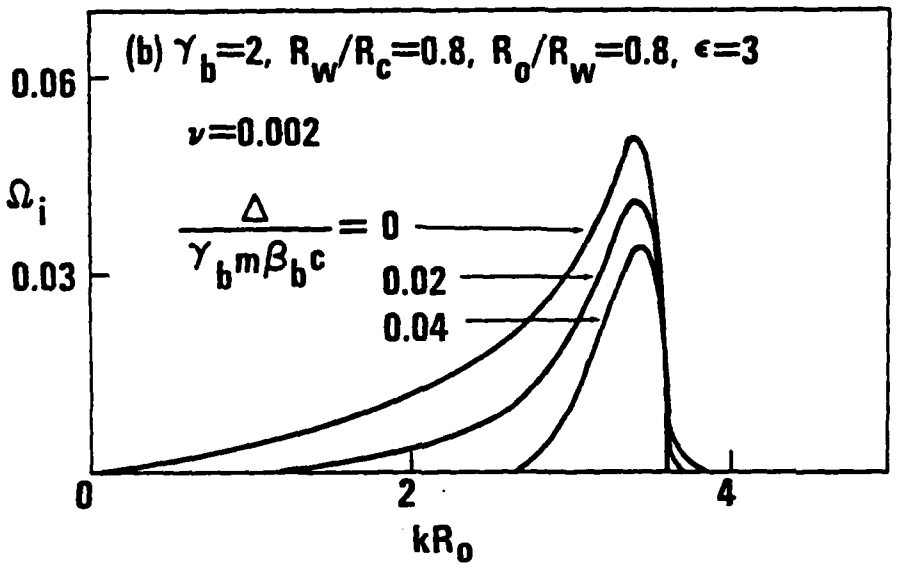

FIGURE 4b THE NORMALIZED GROWTH RATE Ω_i VERSUS kR_0 OBTAINED FROM EQS. (18), (19), (24), AND (32), FOR γ_b = 2, ϵ = 8, R_0/R_w = 0.8, ν = 0.002, AND SEVERAL VALUES OF Δ.

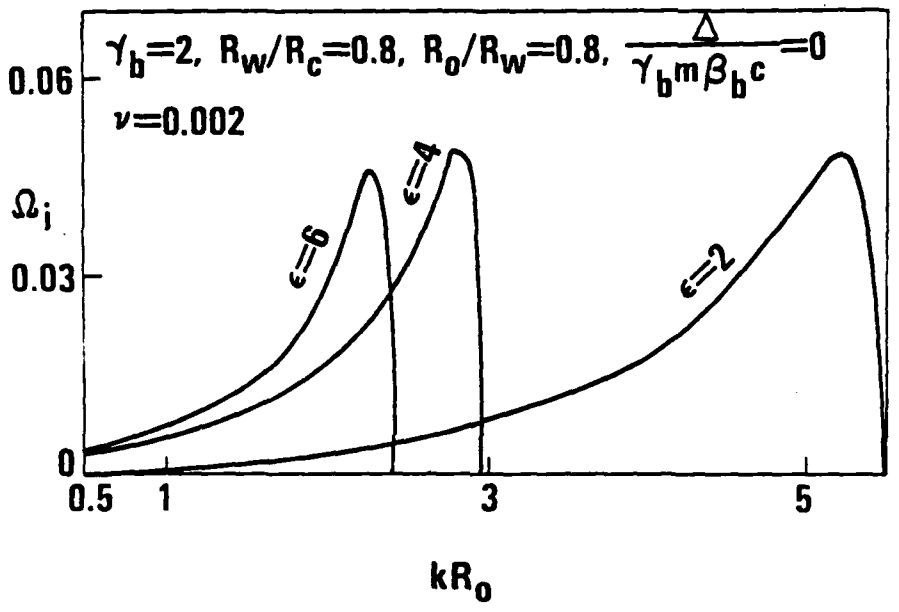

FIGURE 5 PLOT OF THE NORMALIZED GROWTH RATE Ω_i VERSUS kR_0 OBTAINED FROM EQ. (32) FOR $\Delta = 0$, SEVERAL VALUES OF ϵ, AND PARAMETERS OTHERWISE IDENTICAL TO FIG. 4.

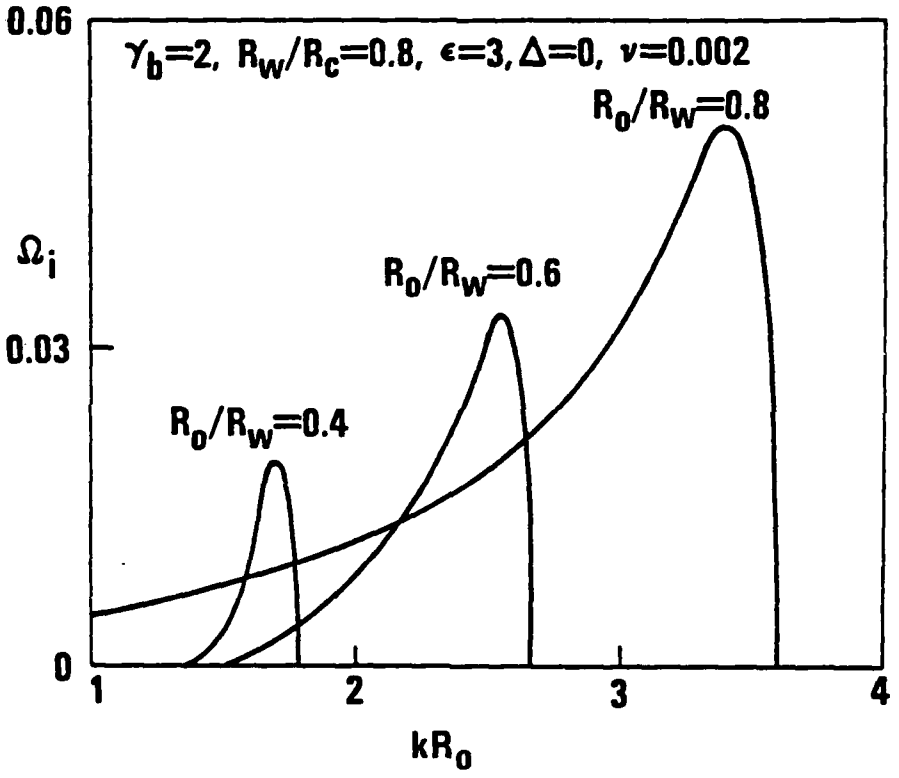

FIGURE 6 PLOT OF THE NORMALIZED GROWTH RATE Ω_j VERSUS kR_0 FOR Δ =0, ϵ = 3, SEVERAL VALUES OF THE RATIO R_0/R_w, AND PARAMETERS OTHERWISE IDENTICAL TO FIG. 4.

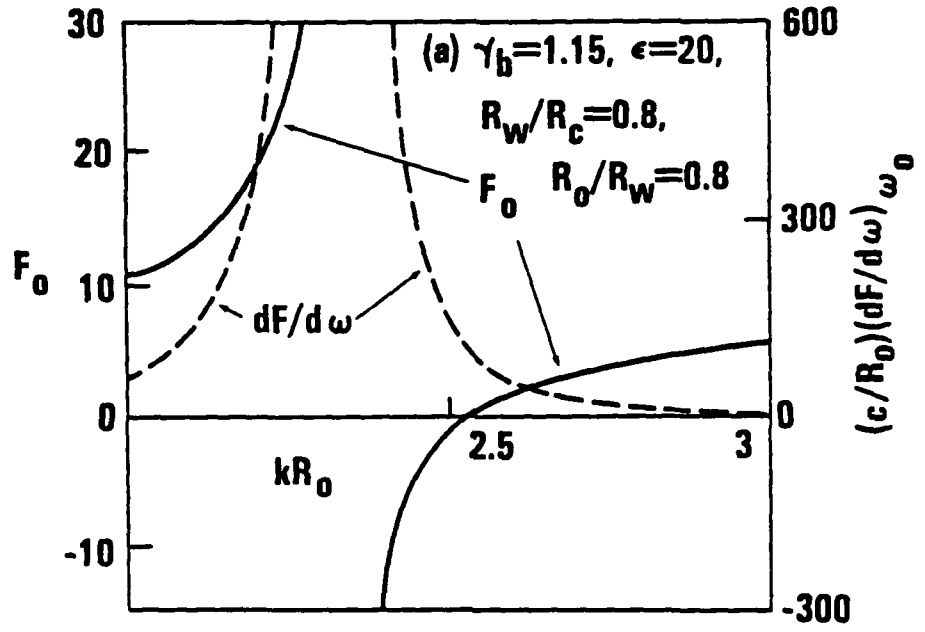

FIGURE 7a PLOT OF (a) F_0 (SOLID CURVE) AND $(c/R_0)\ (dF/d\omega)_{\omega_0}$ (DASHED CURVE).

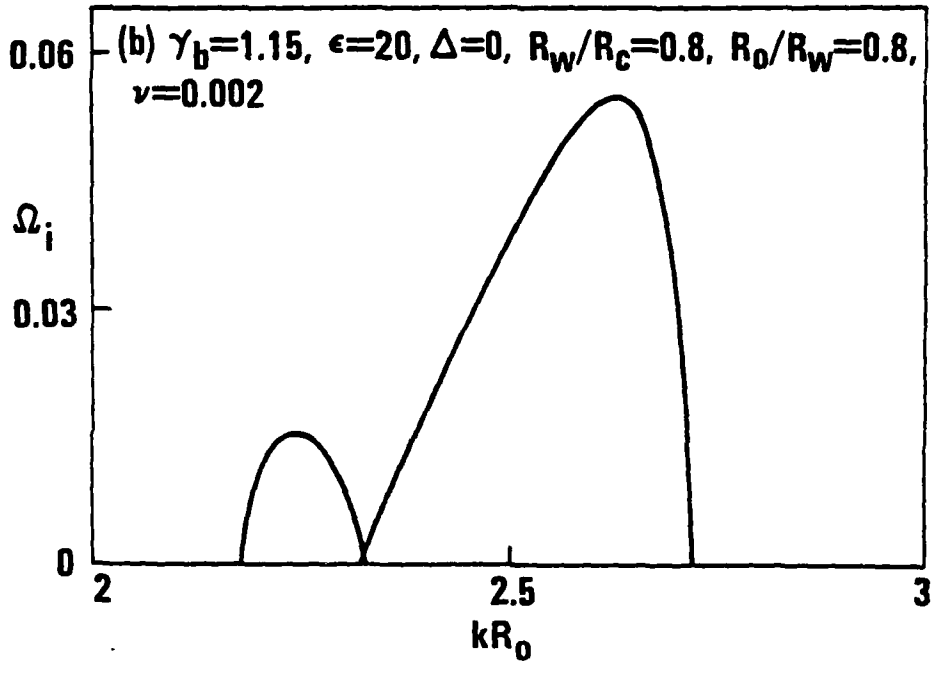

FIGURE 7b THE NORMALIZED GROWTH RATE VERSUS kR_0 OBTAINED FROM EQS. (18), (19), (24), AND (32) FOR $\gamma_b = 1.15$, $\epsilon = 20$, $R_0/R_w = 0.8$, $R_w/R_c = 0.8$, $\Delta = 0$, AND $\nu = 0.002$.

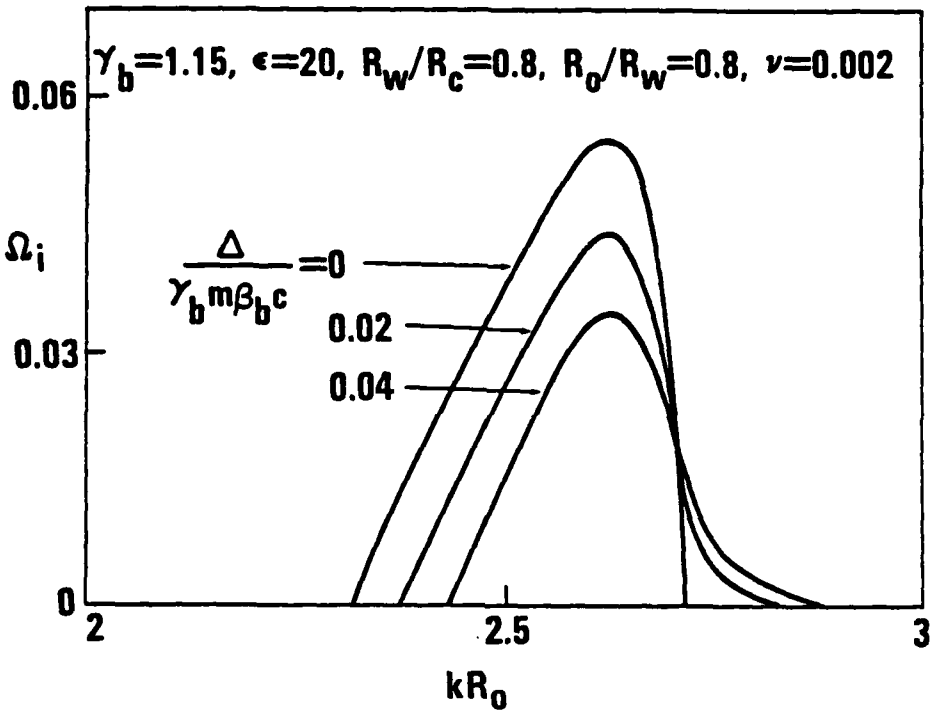

FIGURE 8 PLOT OF THE NORMALIZED GROWTH RATE Ω_i VERSUS kR_0 OBTAINED FROM EQ. (32) FOR SEVERAL VALUES OF Δ, AND PARAMETERS OTHERWISE IDENTICAL TO FIG. 7.

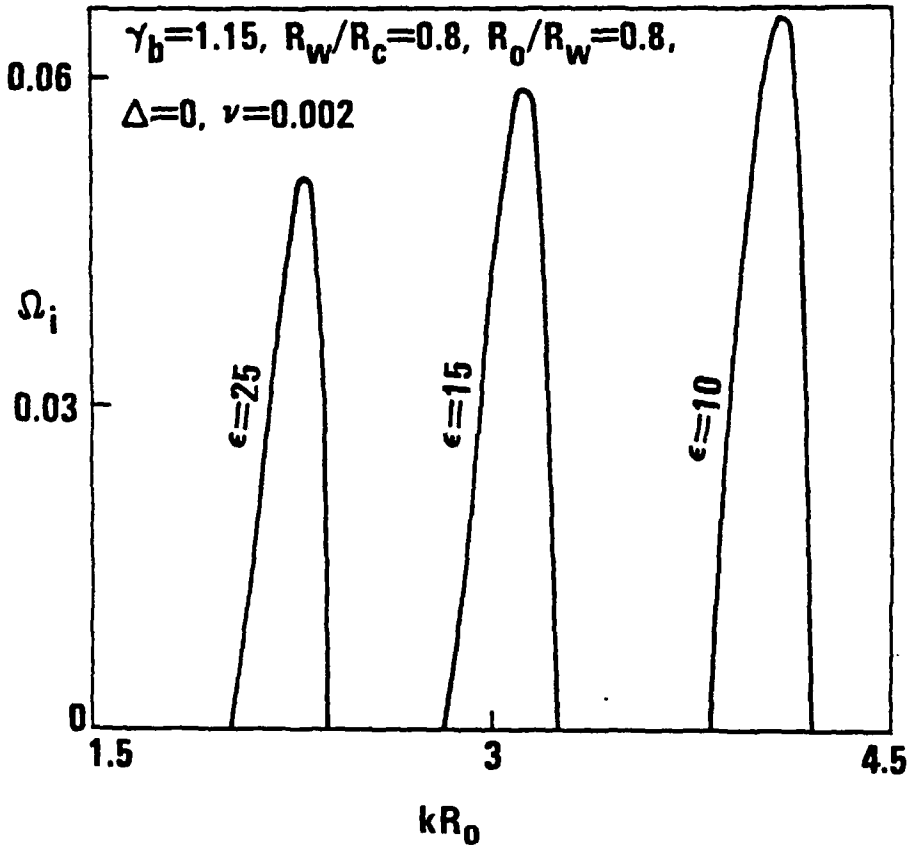

FIGURE 9 PLOT OF THE NORMALIZED GROWTH RATE VERSUS kR_0 FOR Δ = 0, OTHERWISE IDENTICAL TO FIG. 7.

BIBLIOGRAPHY

1. V. A. Flyagin, A. V. Gaponov, M. E. Petelin, and V. K. Yulpatov, IEEE Trans., Microwave Theory Tech. MIT-25, 514 (1977).
2. H. S. Uhm and R. C. Davidson, Phys. Fluids 23, 2538 (1980), and the references therein.
3. G. Bekefi and T. J. Orzechowski, Phys. Rev. Lett. 37, 379 (1976).
4. A. Palevsky and G. Bekefi, Phys. Fluids 22, 986 (1979).
5. D. A. G. Deacon, L. R. Elias, J. M. M. Madey, G. J. Ramian, H. A. Schwettman, and T. I. Smith, Phys. Rev. Lett. 38, 897 (1977).
6. H. S. Uhm, R. C. Davidson, "Theory of Free Electron Laser Instability in a Relativistic Annular Electron Beam", submitted for publication, and the references therein.
7. J. D. Jackson, Classical Electrodynamics (John Wiley & Sons, Inc., New York, 1962), Ch. 14.
8. J. Walsh, D. Kapilow, R. Layman, D. Speer, J. Branscum, D. Wise, and C. Hanna, Bull. Am. Phys. Soc. 25, 949 (1980).

DISTRIBUTION

	Copies
Naval Research Laboratory Attn: Dr. M. Lampe Washington, D. C. 20375	1
Office of Naval Research Attn: W. J. Condell (ONR-421), 800 N. Quincy St. Arlington, Virginia 22217	1
U. S. Army Ballistic Research Laboratory Aberdeen Proving Ground Attn: Dr. D. Eccleshall (DRDAR-BLB) Aberdeen, Maryland 21005	1
Air Force Weapons Laboratory Kirtland Air Force Base Attn: Maj. H. Dogliana Albuquerque, New Mexico 87117	1
Department of Energy Attn: Dr. T. Godlove (C-404) Washington, D. C. 20545	1
National Bureau of Standards Attn: Dr. J. M. Leiss Gaithersburg, Maryland 20760	1
Austin Research Associates, Inc. Attn: Dr. W. E. Drummond 1901 Rutland Drive Austin, Texas 78758	1
Ballistic Missile Defense Advanced Technology Center Attn: Dr. L. J. Harvard (BMDSATC-1) P. O. Box 1500 Huntsville, Alabama 35807	1
B. K. Dynamics, Inc. Attn: Dr. R. Linz 15825 Shady Grove Road Rockville, Maryland 20850	1

DISTRIBUTION (Cont.)

	Copies
The Charles Stark Draper Laboratory, Inc. Attn: Dr. E. Olsson 555 Technology Square Cambridge, Massachusetts 02139	1
Director Defense Advance Research Projects Agency Attn: Dr. J. Mangano 1400 Wilson Boulevard Arlington, Virginia 22209	1
IRT Corporation Attn: Mr. W. Selph P. O. Box 81087 San Diego, California 92138	1
Los Alamos Scientific Laboratory Attn: Dr. G. Best P. O. Box 1663 Los Alamos, New Mexico 87545	1
Mission Research Corporation Attn: Dr. C. Longmire 735 State Street Santa Barbara, California 93102	1
Physical Dynamics, Inc. Attn: Dr. K. Breuckner P. O. Box 977 La Jolla, California 92037	1
Sandia Laboratories Attn: Mail Services Section for: Dr. R. B. Miller Albuquerque, New Mexico 87115	1
Science Applications, Inc. Attn: Dr. M. P. Fricke 1200 Prospect Street La Jolla, California 92037	1
Science Applications, Inc. Attn: Dr. R. Johnston Dr. J. Siambis 2680 Hanover Street Palo Alto, California 94304	1 1

DISTRIBUTION (Cont.)

	Copies
University of California Lawrence Livermore Laboratory Attn: Dr. R. J. Briggs Dr. E. Lee P. O. Box 808 Livermore, California 94550	 1 1
Defense Technical Information Center Cameron Station Alexandria, Virginia 22314	12
Naval Sea Systems Command Washington, D. C. 20362 Attn: SEA-09G32 SEA-03B	 2 1

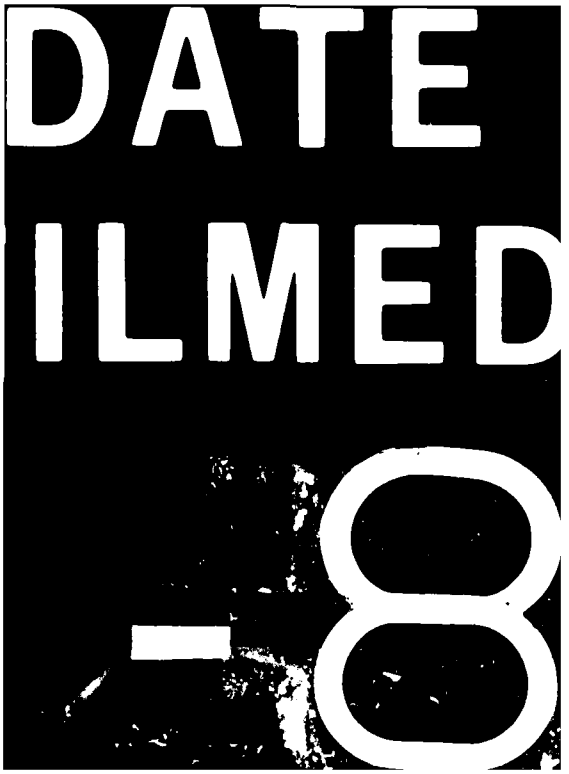
DATE
ILMED
-8